RECENT RESULTS ON CP VIOLATION AND RARE DECAYS FROM LHCb*

Michał Kazanecki

on behalf of the LHCb Collaboration

Institute of Nuclear Physics Polish Academy of Sciences, 31-342 Kraków, Poland

Received 12 April 2025, accepted 16 April 2025, published online 26 June 2025

The LHCb experiment at CERN's Large Hadron Collider is dedicated to studying heavy-flavour physics, particularly the decays and properties of beauty and charm hadrons, to explore CP violation and phenomena beyond the Standard Model. This contribution presents a selection of recent measurements in rare decays and CP violation.

DOI:10.5506/APhysPolBSupp.18.5-A13

1. Introduction

The LHCb experiment plays a crucial role in testing the limits of the Standard Model (SM) by studying rare decays and CP violation in heavy quarks. Rare decays, which occur through flavour changing neutral currents (FCNC) are heavily suppressed in the SM, and are very sensitive to New Physics (NP) contributions. CP violation, which describes differences in behaviour between matter and antimatter, is essential for understanding matter–antimatter asymmetry in our universe.

The LHCb detector [1] is a single-arm forward spectrometer, designed for the study of particles containing b or c quarks. It has an excellent tracking, vertexing, and particle identification system. Different types of charged hadrons are distinguished using information from ring-imaging Cherenkov detectors. Photons, electrons, and hadrons are identified by a calorimeter system. Muons are identified by muon stations.

The reconstruction and selection of events is performed by a trigger, which in Run 2 consisted of a hardware stage based on information from the calorimeter and muon systems, followed by a software stage, which applies a full event reconstruction. LHCb has collected large samples of pp collisions, corresponding to an integrated luminosity of 3 fb^{-1} in Run 1 and 6 fb^{-1} in Run 2.

* Presented at the 31$^{\rm st}$ Cracow Epiphany Conference on the *Recent LHC Results*, Kraków, Poland, 13–17 January, 2025.

2. Rare beauty decays

Decays mediated by the $b \to s\ell^+\ell^-$ transition are suppressed in the Standard Model due to the absence of flavour changing neutral currents at tree level and they are sensitive to contributions from physics beyond the Standard Model (BSM). Previous studies revealed tensions with SM predictions in branching fractions and angular observables [2].

Theoretically, these decays can be described in the Weak Effective Theory (WET) framework [3], encapsulated by the Hamiltonian

$$\mathcal{H}_{\mathrm{WET}} = \frac{-4G_{\mathrm{F}}}{\sqrt{2}} V_{ts}^* V_{tb} \sum_i \mathcal{C}_i^{(\prime)}(\mu)\mathcal{O}_i^{(\prime)}(\mu)\,, \tag{1}$$

where G_{F} is the Fermi constant and $V_{q_k q_j}$ are elements of the Cabibbo–Kobayashi–Maskawa (CKM) matrix. The operators $\mathcal{O}_i^{(\prime)}$ arise from integrating out all heavy degrees of freedom, and the Wilson Coefficients $\mathcal{C}_i^{(\prime)}$ are the corresponding effective coupling constants.

In angular analyses, decay can be described by 3 angles and 8 parameters depending on the dilepton invariant mass squared (q^2)

$$\begin{aligned}
&\frac{1}{\mathrm{d}\left(\mathit{\Gamma}+\bar{\mathit{\Gamma}}\right)/\mathrm{d}q^2}\frac{\mathrm{d}^4\left(\mathit{\Gamma}+\bar{\mathit{\Gamma}}\right)}{\mathrm{d}q^2\mathrm{d}\vec{\mathit{\Omega}}} = \frac{9}{32\pi}\left[\frac{3}{4}(1-F_{\mathrm{L}})\sin^2\theta_K + F_{\mathrm{L}}\cos^2\theta_K\right. \\
&+\frac{1}{4}(1-F_{\mathrm{L}})\sin^2\theta_K\cos 2\theta_\ell - F_{\mathrm{L}}\cos^2\theta_K\cos 2\theta_\ell + S_3\sin^2\theta_K\sin^2\theta_\ell\cos 2\phi \\
&+S_4\sin 2\theta_K\sin 2\theta_\ell\cos\phi + S_5\sin 2\theta_K\sin\theta_\ell\cos\phi + \frac{4}{3}A_{\mathrm{FB}}\sin^2\theta_K\cos\theta_\ell \\
&\left.+S_7\sin 2\theta_K\sin\theta_\ell\sin\phi + S_8\sin 2\theta_K\sin 2\theta_\ell\sin\phi + S_9\sin^2\theta_K\sin^2\theta_\ell\sin 2\phi\right],
\end{aligned} \tag{2}$$

where F_{L} is the fraction of longitudinally polarised K^{*0} mesons, A_{FB} is the forward–backward asymmetry of the dilepton system, and S_i are the other CP-averaged S-basis observables. The S-basis observables can be used to construct a set of optimised P-basis observables, for which form-factor uncertainties cancel at leading order [4], for example

$$P_5' = \frac{S_5}{\sqrt{F_{\mathrm{L}}(1-F_{\mathrm{L}})}}\,. \tag{3}$$

2.1. Angular analysis of $B^0 \to K^{*0}\mu^+\mu^-$

The matrix element for $B^0 \to K^{*0}\mu^+\mu^-$ decay has components related to both local and non-local contributions [5]. The leading non-local contributions are due to narrow charmonium resonances but influence all parts of the phase space. The non-local contributions can have significant effects far away from the resonances through interference. Such effects lead to a shift in $\mathcal{C}_9$ that can potentially be large enough to resolve the observed tensions in the angular observables without requiring any New Physics affecting the local contributions.

A novel feature of this analysis is to include the full phase space and determine the local and non-local contributions simultaneously. In this way the theoretical model dependence related to the non-local contributions is reduced as they are determined directly from the data.

Most of the obtained Wilson coefficients are consistent with the SM predictions, while for $\mathcal{C}_9$, there is 2.1σ deviation observed (Fig. 1).

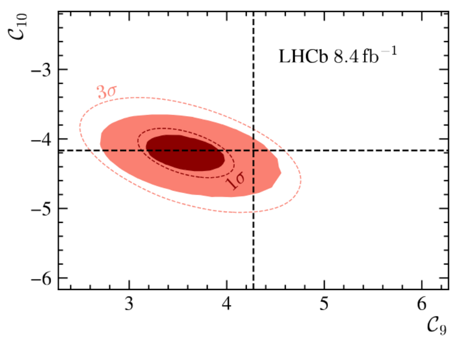

Fig. 1. Two-dimensional confidence regions for $\mathcal{C}_9$ and $\mathcal{C}_{10}$ Wilson coefficients.

Role of the non-local contributions in the observable P_5' is presented in Fig. 2. The total observable with SM values of Wilson coefficients have central values closer to those of the data fit results, indicating that the data prefer larger non-local contributions than the formal SM predictions.

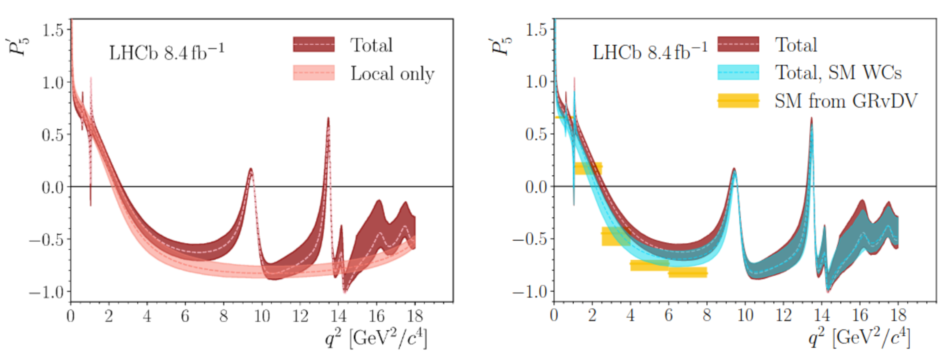

Fig. 2. Distributions of the observable P_5' constructed out of the signal parameters from the baseline fit to data.

Nevertheless, these values are different from the baseline fit and are closer to the SM predictions, which indicates that the non-local contributions are not sufficient to explain the shift in $\mathcal{C}_9$.

2.2. Angular analysis of $B^0 \to K^{*0}e^+e^-$

The analysis was performed in the central q^2 region of 1.1–6.0 GeV^2/c^4. The aim of the analysis was to determine angular observables and test lepton flavour universality (LFU) in the angular distribution [6].

The angular observables of the decay, are shown in Fig. 3 together with the SM predictions. The overall set of angular observables shows good agreement with the SM predictions, however, the small discrepancies observed in F_{L} and A_{FB} are coherent with the hypothesis of a negative shift in the value of Wilson coefficient $\mathcal{C}_9$.

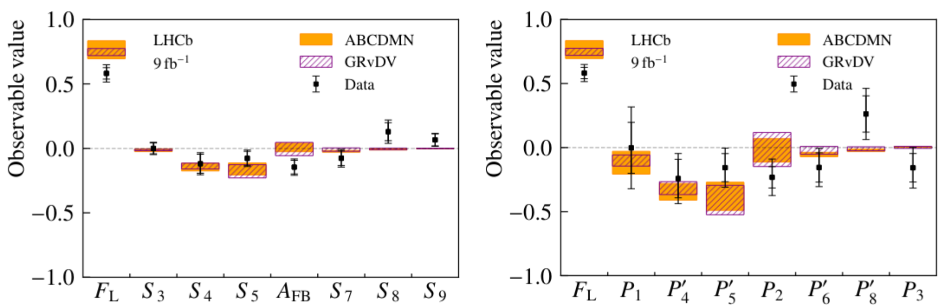

Fig. 3. The (left) S- and (right) P-basis angular observables.

The LFU angular observables $Q_i = P_i^{(\mu)} - P_i^{(e)}$ are summarised in Fig. 4. Most of them show good agreement with the LFU hypothesis. The largest difference is found for Q_{FL} at the level of 1.9σ.

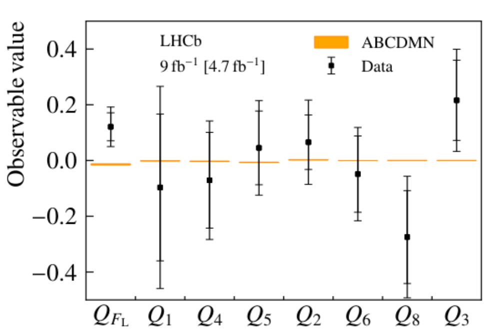

Fig. 4. LFU observables Q_i calculated using the P-basis angular observables of the muon and electron modes.

2.3. Angular analysis of $B_s^0 \to \phi e^+e^-$

In the SM, the electroweak charged current has chiral interactions, coupling to left-handed quarks. As a result, in the $b \to s\gamma$ transitions, photons are mostly left-handed, with a small right-handed contribution that has a relative amplitude proportional to the mass ratio of the s-to-b quark. The presence of a significant right-handed polarisation would be a clear signature of the BSM physics [7].

The very low-q^2 region (between 0.0009 and 0.2615 GeV^2/c^4) is fundamental for the determination of the $\mathcal{C}_7$ and $\mathcal{C}_7'$ Wilson coefficients and photon polarisation. $b \to se^+e^-$ transition is particularly sensitive to the photon pole due to the smallness of the electron mass.

The total signal yield, observed within the effective q^2 range, is about 100 events. It is the first observation of the $B_s^0 \to \phi e^+e^-$ decay (together with [8]). Angular observables were used to measure both the real and imaginary parts of the $B_s^0 \to \phi\gamma$ photon polarisation with a precision of 12% (Fig. 5). All results are with agreement with SM predictions.

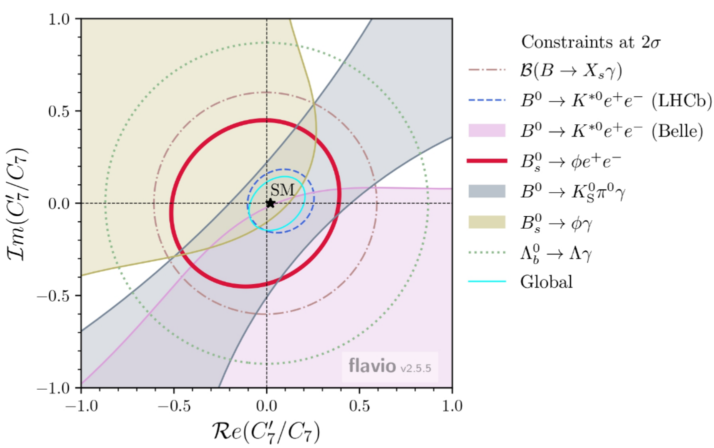

Fig. 5. Current constraints at the 2σ level on the real and imaginary part of the ratio of the right- to left-handed Wilson coefficients $\mathcal{C}_7'$ and $\mathcal{C}_7$.

2.4. Tests of LFU using $B_s^0 \to \phi\ell^+\ell^-$

The analysis [8] is the first measurement of the lepton universality ratio of branching fractions $R_\phi = \mathcal{B}(B_s^0 \to \phi\mu^+\mu^-)/\mathcal{B}(B_s^0 \to \phi e^+e^-)$. In practice, R_ϕ^{-1} is measured rather than R_ϕ such that the small electron yield appears in the numerator and the statistical behaviour of the observable more closely follows a Gaussian distribution.

One advantage of performing tests with $B_s^0 \to \phi\ell^+\ell^-$ decays is the clean signature of the $\phi \to K^+K^-$ decay, which significantly reduces most sources of background.

The statistical significance of the $B_s^0 \to \phi e^+e^-$ signal in low-, central-, and high-q^2 bins correspond to 6.8σ, 5.4σ, and 3.6σ, respectively. Figure 6 shows the variation with R_ϕ^{-1} of the difference in log-likelihood of the fit from the best-fit point. The results agree with the SM expectation of lepton flavour universality.

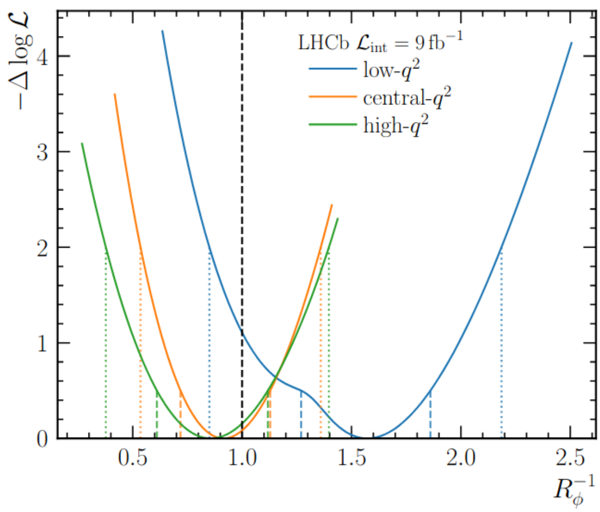

Fig. 6. Profile log-likelihood of R_ϕ^{-1} for the low-, central-, and high-q^2 bins, relative to the best-fit point. The black vertical line shows SM prediction.

3. Rare charm decays

Rare charm decays may proceed via FCNC $c \to u\ell^+\ell^-$ transitions which are equivalent to $b \to s\ell^+\ell^-$ transitions. In the SM, short-distance contributions for this type of decays result in branching fractions of $\mathcal{O}(10^{-9})$ [9]. Long-distance processes involving intermediate hadronic resonances increase branching fractions up to $\mathcal{O}(10^{-6})$. Despite the dominance of long-distance contributions, the effects of NP may lead to deviations from the SM predictions.

3.1. *Search for $D^0 \to h^+h^-e^+e^-$ decays*

The decay of $D^0 \to h^+h^-e^+e^-$ offers the opportunity for the first lepton universality test as muon modes of the decays were observed before at the LHCb [10].

The analysis [11] was performed in 5 dilepton mass regions defined according to the presence of known intermediate resonances. The $D^0 \to \pi^+\pi^-e^+e^-$ decay was observed for the first time in ρ^0/ω and ϕ regions. Branching fractions in these regions are found to be $\mathcal{B} = (4.5 \pm 1.0 \pm 0.7 \pm 0.6) \times 10^{-7}$ and $\mathcal{B} = (3.8 \pm 0.7 \pm 0.4 \pm 0.5) \times 10^{-7}$ respectively. Comparison of electron and muon results confirm lepton universality at the current precision. No evidence was found for the $D^0 \to K^+K^-e^+e^-$ decay.

3.2. Search for $\Lambda_c^+ \to p\mu^+\mu^-$ decays

The analysis [12] was carried out in six regions of dimuon invariant mass. The non-resonant signal decay was searched for in two regions, *low-m* ($211.32 < m_{\mu\mu} < 507.86$) and *high-m* ($1059.46 < m_{\mu\mu} < 1348.13$), where the expected contributions of resonances were subdominant and ϕ resonant region was used for normalisation.

In the high-mass region, signal yield significance is close to but lower than 3σ, while in the *low-m* region, no signal was found. Excluding the normalization channel, the significance of the Λ_c signal exceeds the 5σ threshold in the ρ and ω regions, while the significance in η region is at the 3σ level.

The value of the upper limit extrapolated from the signal region to the full phase was found to be $\mathcal{B}(\Lambda_c^+ \to p\mu^+\mu^-) < 7.3\,(8.2) \times 10^{-8}$ at 90% (95%) C.L. (Fig. 7). In spite of the enlarged data sample, the extrapolated upper limit on the branching fraction is only slightly better than the one determined for Run 1 [13], this is driven mainly by the 2.8σ effect observed in the *high-m* region.

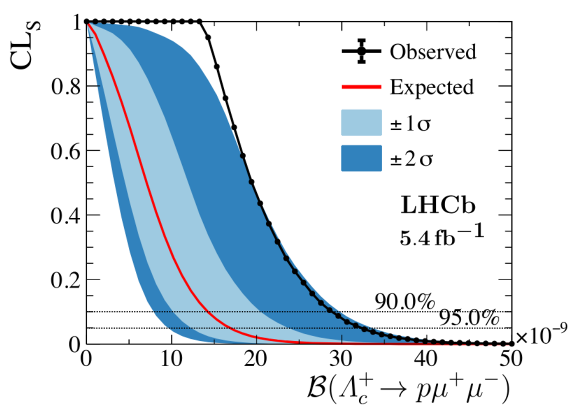

Fig. 7. Observed and expected (background only hypothesis) limits for the $\Lambda_c^+ \to p\mu^+\mu^-$ branching fraction.

4. CP violation

4.1. CP asymmetry and branching fraction of $B^+ \to J/\psi\pi^+$ decays

Beauty decays to charmonium final states play a pivotal role in the study of CP violation. In general, CP violation can arise directly from the interference of the leading-order tree amplitude and the loop (penguin) amplitudes of such decays.

An open issue in the weak phases determination is related to the effects of the subleading contributions from highly-suppressed penguin diagrams in $b \to c\bar{c}s$ transitions, which need to be fully understood for more precise tests of the SM. Such effects can be controlled with measurements of $b \to c\bar{c}d$ transitions where penguin contributions are less CKM-suppressed [14].

The presented analysis [15] is a new measurement of CP asymmetry $\Delta\mathcal{A}^{\mathrm{CP}}$ and branching fraction of $B^+ \to J/\psi\pi^+$ decay with Run 2 data. In order to subtract the small difference between the production cross sections of B^- and B^+ mesons, the asymmetry is measured with respect to control sample of $B^+ \to J/\psi K^+$ decay, where direct CP violation is expected to be negligible. Information on the penguin contributions can be obtained from the ratio of branching fractions $\mathcal{R}_{\pi/K} = \mathcal{B}(B^+ \to J/\psi\pi^+)/\mathcal{B}(B^+ \to J/\psi K^+)$, where the systematic uncertainties largely cancel out.

Figure 8 shows the comparison of the branching fraction ratio and $\Delta\mathcal{A}^{\mathrm{CP}}$ measurements from Run 1, 2016, 2017, and 2018 data and the average values. It is the most precise measurement of the CP-asymmetry difference between $B^+ \to J/\psi\pi^+$ and $B^+ \to J/\psi K^+$ decays.

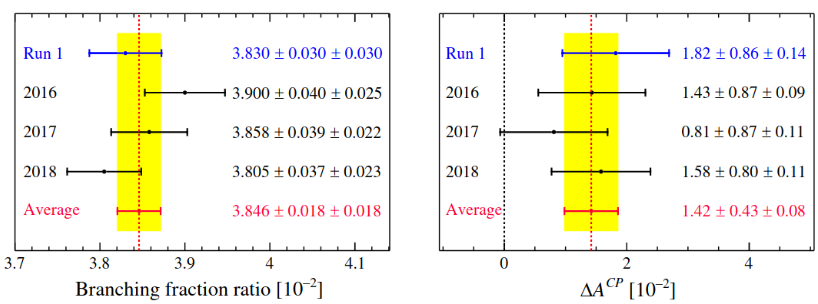

Fig. 8. Comparison of the $\mathcal{R}_{\pi/K}$ and $\Delta\mathcal{A}^{\mathrm{CP}}$ measurements from Run 1, 2016, 2017, and 2018 data and the average values.

The combined CP asymmetry difference shows a 3.2σ deviation from zero, which is the first evidence of direct CP violation in beauty decays to charmonium final states. The $\Delta\mathcal{A}^{\mathrm{CP}}$ and $\mathcal{R}_{\pi/K}$ measurements serve to set constraints on the size and strong phase of penguin-to-tree contribution ratio assuming SU(3) flavour symmetry.

4.2. Study of Λ_b^0 and Ξ_b^0 decays to $\Lambda h^+ h'^-$ final states

In three-body charmless B-meson decays, large CPV is observed in localized regions of phase space [16], which suggests that resonance interactions and $\pi^+\pi^- \leftrightarrow K^+K^-$ rescattering play an important role in the generation of strong phases. This motivates studies of Λ_b^0 and Ξ_b^0 decays to $\Lambda h^+ h'^-$final states, which are governed by similar dynamics in the SM.

In the study of [17], measurements of branching fractions and CP asymmetries for charmless decays of Λ_b^0 and Ξ_b^0 into the final states $\Lambda K^\pm \pi^\mp$, $\Lambda K^+ K^-$, and $\Lambda \pi^+\pi^-$ were performed.

The significances of the $\Lambda_b^0 \to \Lambda\pi^+\pi^-$ and $\Xi_b^0 \to \Lambda K^-\pi^+$ decays are measured to be more than 10σ, giving the first observation of these decays. Significance of the $\Xi_b^0 \to \Lambda\pi^+\pi^-$ decay is 4σ which gives its first evidence.

CPV was investigated in four channels with sufficient yields. The CP asymmetry for $\Lambda_b^0 \to \Lambda K^+ K^-$ was found to be $\Delta\mathcal{A}^{\mathrm{CP}} = (8.3 \pm 2.8)\%$ which is the first evidence of direct CPV in this decay. The decay is dominated by intermediate N^{*+} or ϕ resonances (Fig. 9). The CP asymmetry in the N^{*+} mass region is enhanced to $\Delta\mathcal{A}^{\mathrm{CP}} = (16.5 \pm 5.1)\%$. This result, if confirmed, can provide useful insight into sources of CPV in barion dynamics.

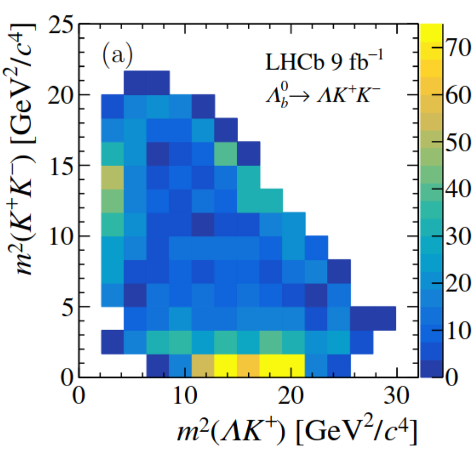

Fig. 9. Dalitz plots of the $\Lambda_b^0 \to \Lambda K^+ K^-$ decay.

4.3. Mixing and CPV in charm decays

Mixing in charm hadrons is especially suppressed in comparison with strange and beauty systems by the corresponding CKM matrix elements. The $D^0(t) \to K^+\pi^-$ decay is an excellent candidate to study oscillations as it receives contributions from interfering amplitudes of comparable magnitudes from the doubly Cabibbo-suppressed $D^0 \to K^+\pi^-$ decay and from the Cabibbo-favoured $\bar{D}^0 \to K^+\pi-$ decay following a D^0–$\bar{D}^0$ oscillation. Analysis of the time evolution of the ratios of the decay rates

$$R^+_{K\pi}(t) = \frac{\Gamma\left(D^0(t) \to K^+\pi^-\right)}{\Gamma\left(\bar{D}^0(t) \to K^+\pi^-\right)}$$

and

$$R^-_{K\pi}(t) = \frac{\Gamma\left(\bar{D}^0(t) \to K^-\pi^+\right)}{\Gamma\left(D^0(t) \to K^-\pi^+\right)}$$

is sensitive to both mixing parameters and CPV [18].

The analysis provides the most precise D^0–$\bar{D}^0$ mixing measurement. Figure 10 shows half the sum and half the difference of the decay rate ratios. The results are compatible with the hypothesis of CP symmetry. Additional constraints come from complementary analysis performed recently with D^0 coming from semileptonic B decays [19].

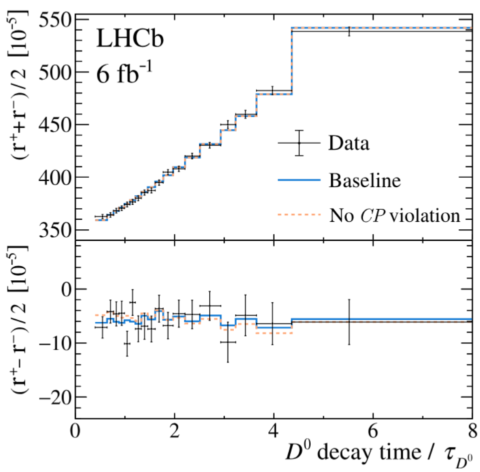

Fig. 10. Half the sum and half the difference of measured decay rate ratios as a function of decay time.

5. Summary

Comprehensive studies of rare beauty and charm decays were performed, testing lepton flavour universality, angular observables, and CP violation. While most results align with the Standard Model predictions, the tension observed in $b \to sll$ decays is still present and its origin is not known. In Run 3, a large increase in sample size is expected which opens the door to even more precise measurements.

REFERENCES

[1] LHCb Collaboration (A.A. Alves, Jr. *et al.*), *J. Instrum.* **3**, S08005 (2008).
[2] LHCb Collaboration (R. Aaij *et al.*), *J. High Energy Phys.* **2013**, 131 (2013).
[3] W. Altmannshofer *et al.*, *J. High Energy Phys.* **2009**, 019 (2009).
[4] S. Descotes-Genon, T. Hurth, J. Matias, J. Virto, *J. High Energy Phys.* **2013**, 137 (2013).
[5] LHCb Collaboration (R. Aaij *et al.*), *J. High Energy Phys.* **2024**, 026 (2024).
[6] LHCb Collaboration (R. Aaij *et al.*), `arXiv:2502.10291 [hep-ex]`.
[7] LHCb Collaboration (R. Aaij *et al.*), *J. High Energy Phys.* **2025**, 047 (2025).
[8] LHCb Collaboration (R. Aaij *et al.*), *Phys. Rev. Lett.* **134**, 121803 (2025).
[9] A. Paul, I.I. Bigi, S. Recksiegel, *Phys. Rev. D* **83**, 114006 (2011).
[10] LHCb Collaboration (R. Aaij *et al.*), *Phys. Rev. Lett.* **119**, 181805 (2017).
[11] LHCb Collaboration (R. Aaij *et al.*), `arXiv:2412.09414 [hep-ex]`.
[12] LHCb Collaboration (R. Aaij *et al.*), *Phys. Rev. D* **110**, 052007 (2024).
[13] LHCb Collaboration (R. Aaij *et al.*), *Phys. Rev. D* **97**, 091101 (2018).
[14] K. De Bruyn, R. Fleischer, *J. High Energy Phys.* **2015**, 145 (2015).
[15] LHCb Collaboration (R. Aaij *et al.*), *Phys. Rev. Lett.* **134**, 101801 (2025).
[16] LHCb Collaboration (R. Aaij *et al.*), *Phys. Rev. D* **108**, 012008 (2023).
[17] LHCb Collaboration (R. Aaij *et al.*), *Phys. Rev. Lett.* **134**, 101802 (2025).
[18] LHCb Collaboration (R. Aaij *et al.*), *Phys. Rev. D* **111**, 012001 (2025).
[19] LHCb Collaboration (R. Aaij *et al.*), *J. High Energy Phys.* **2025**, 149 (2025).